

# Metastasis-associated protein 2 promotes the metastasis of non-small cell lung carcinoma by regulating the ERK/AKT and VEGF signaling pathways

BIN ZHANG<sup>1</sup>, FENG TAO<sup>2</sup> and HAO ZHANG<sup>1</sup>

<sup>1</sup>Department of Respiratory Disease, The Second Affiliated Hospital, Zhejiang University College of Medicine, Hangzhou, Zhejiang 120070; <sup>2</sup>Department of Respiratory Disease, The First Hospital of Jiaxing, Jiaxing, Zhejiang 320090, P.R. China

Received August 24, 2016; Accepted May 23, 2017

DOI: 10.3892/mmr.2018.8535

**Abstract.** Non-small cell lung carcinoma (NSCLC) is the most common cause of cancer-associated mortality in the world and accounts for ~85% of human lung cancers. Metastasis-associated protein 2 (MTA2) is a component of the histone deacetylase complex and serves a role in tumor progression; however, the mechanism through which MTA2 is involved in the progression of NSCLC remains unclear. The aim of the present study was to investigate the expression and function of MTA2 and the MTA2-mediated signaling pathway in NSCLC cells. Expression of MTA2 and its target genes was analyzed in MTA2-overexpressing and anti-MTA2 antibody (AbMTA2)-treated NSCLC cells, as well as growth, migration, invasion and apoptotic-resistance. The inhibitory effects on tumor formation were analyzed using AbMTA2-treated NSCLC cells and in a mouse model. Histological assessment was conducted to analyze the expressions levels of extracellular signal-regulated kinase (ERK), RAC- $\alpha$  serine/threonine protein kinase (AKT) and vascular endothelial growth factor (VEGF) in experimental tumors. Results of the present study demonstrated that MTA2 was overexpressed in NSCLC cells. The growth, migration and invasion of NSCLC cells were markedly inhibited by AbMTA2. In addition, it was observed that the ERK/AKT and VEGF signaling pathways were both upregulated in MTA2-overexpressing NSCLC cells, and downregulated following silencing of MTA2 activation. ERK and AKT phosphorylation levels were downregulated in NSCLC cells and tumors following MTA2 silencing. The *in vivo* study demonstrated that tumor growth was markedly

inhibited following siRNA-MTA2 treatment. In conclusion, the results of the present study suggested that MTA2 silencing may significantly inhibit the growth and aggressiveness of NSCLC cells. Results from the present study indicated that the mechanism underlying the MTA2-mediated invasive potential of NSCLC cells involved the ERK/AKT and VEGF signaling pathways, which may be a potential therapeutic target for the treatment of NSCLC.

## Introduction

Lung cancer is an important public health concern and the leading cause of cancer-associated mortality worldwide (1). Pathological findings have indicated that lung cancer is a respiratory disease that may be associated with air contamination caused by industrial pollution (2). Non-small cell lung carcinoma (NSCLC) and small cell lung carcinoma are the two types of lung cancer, with incidence rates of ~85% and ~15%, respectively, according to a clinical statistical analysis of human cancers (3). NSCLCs include large-cell carcinoma, squamous cell carcinoma and adenocarcinoma, the incidences of which are increasing (4-6). NSCLC represents ~85% of all cases of lung cancer and results in a subsequently high mortality rate (7). NSCLC is initiated from the non-small cells in the lung, and is the most common type of cancer worldwide (8). According to clinical statistical investigations into lung cancer, >80% of newly diagnosed patients are in the middle or severe stages of the disease (9-11).

Although continuing investigations have sought to improve the efficacy of treatment for patients with NSCLC, the 5-year survival rate remains poor at <15% (5,12,13). In addition, the majority of newly diagnosed patients with NSCLC are at an advanced stage, contributing to the high mortality rate (14,15). Previous studies have reported that the migration and invasion of NSCLC cells are the primary causes of the poor survival rate during treatment and the rate of recurrence for patients with NSCLC (16,17). As a result, the development of effective agents that inhibit migration and invasion has become a necessity for the treatment of patients with cancer (18,19).

Radiotherapy, chemotherapy and other treatments used in patients with locally advanced NSCLC have been

**Correspondence to:** Professor Hao Zhang, Department of Respiratory Disease, The Second Affiliated Hospital, Zhejiang University College of Medicine, 88 Jiefang Road, Hangzhou, Zhejiang 120070, P.R. China

E-mail: zhanghaoedu@126.com

**Key words:** non-small cell lung carcinoma, metastasis-associated protein 2, extracellular signal-regulated kinase, RAC- $\alpha$  serine/threonine protein kinase, vascular endothelial growth factor

demonstrated to improve outcomes more effectively than up-front surgical resection (20-22). These conventional therapies have been demonstrated to be effective at temporarily controlling the disease (23,24); however, previous studies on nasopharyngeal carcinoma have demonstrated that high-dose irradiation and/or chemical drugs may be associated with an increased probability of toxicity and damage to the immune system, which led to more rapid migration and invasion (25-27). A number of previous studies have proposed more advanced oncotherapeutic techniques to improve patient outcomes, including virotherapy, immunotherapy, targeted therapy, stem cell therapy, gene therapy and comprehensive care (28-31). According to previous analyses of therapeutic efficacy, targeted therapy exhibits the potential for human cancer treatment and the possibility of eradicating tumor cells; for example, a tumor-free condition was attained by targeting the digoxin-specific antigen of tumor cells (32,33).

Metastasis-associated protein 2 (MTA2) is a member of the MTA family of chromatin remodeling proteins, which have been reported to serve roles in tumor progression and metastasis (34,35). Previous studies have demonstrated that MTA2 is overexpressed in a number of cancers, which indicated that the inhibition of MTA2 activity may be beneficial for the treatment of human cancer (36,37). Additional studies have indicated that MTA2 may be required for the invasion and metastasis of human pituitary adenomas through the epithelial-mesenchymal transition pathway, and overexpression of MTA2 may contribute to breast cancer cell growth, resulting in an enhanced anchorage-independent growth and metastasis (38,39). In addition, MTA2 has been associated with bone invasion and tumor stage in human pituitary adenomas (40). These previous reports suggested that MTA2 may be a potential target for inhibiting tumor growth and aggressiveness in the treatment of cancer.

The present study investigated the expression and function of MTA2 and MTA2-mediated signaling in NSCLC cells. Although our previous study suggested that MTA2 may promote the metastasis of NSCLC by inhibiting the expression of epithelial cell adhesion molecule (Ep-CAM) and E-cadherin, the mechanisms of MTA2-mediated signaling pathway have not been elucidated in NSCLC cells (41). The results of the present study demonstrated that the extracellular signal-regulated kinase (ERK) and RAC- $\alpha$  serine/threonine protein kinase (AKT) signaling pathways may be involved in the progression of MTA2-mediated migration and invasion of NSCLC cells. Additionally, the inhibitory effects of MTA2-mediated tumor growth were analyzed *in vitro* and *in vivo*.

## Materials and methods

**Ethics statement.** The present study was performed in accordance with the recommendations in The Guide for the Care and Use of Laboratory Animals of Tianjin Medical University (Tianjin, China). Experimental protocols were approved by The Chinese Association for Laboratory Animal Science (Beijing, China). All surgeries and euthanasia were performed under sodium pentobarbital anesthesia, and all efforts were made to minimize suffering.

**Cell culture and reagents.** A549 and H358 human lung carcinoma cells were purchased from The American Type Culture Collection (ATCC; Manassas, VA, USA). A549 and H358 cells were cultured in RPMI-1640 medium (Gibco; Thermo Fisher Scientific, Inc., Waltham, MA, USA) supplemented with 10% heat-inactivated FBS (Gibco; Thermo Fisher Scientific, Inc.), 3 mM L-glutamine, 50  $\mu$ g/ml gentamicin (BioWhittaker; Lonza Group, Ltd., Basel, Switzerland) and 1% penicillin/streptomycin. The MRC-5 (no. 55-X<sup>TM</sup>; ATCC) normal lung cell line were cultured in minimum essential medium (MEM; Gibco; Thermo Fisher Scientific, Inc.) supplemented with 10% heat-inactivated FBS. Cells were cultured at 37°C with 5% CO<sub>2</sub>. All cells were demonstrated to be free from mycoplasma contamination.

**Transfection of micro (mi)RNA mimics and small interfering (si)RNA.** All siRNAs were synthesized by Invitrogen (Thermo Fisher Scientific, Inc.), including si-MTA2 and siRNA-control (si-MTA2 sense strand, 5'-UGAACAAGACAGAGCUCA ATT-3' and antisense strand, 5'-UUGAGCUCUGUCUUGU UCATT-3'; siRNA-control sense strand, 5'-UGAUGAUCC A CCAAGAGCUCUUGCC-3' and antisense strand, 5'-UUG AGCUCUGUCUUGUUCATT-3'; miMTA2 sense strand, 5'-CACTCGAGAGTCCACCTCCAGTGTAGdTdT-3' and antisense strand, 3'-dTdTTCAGCGGCCGCAGTCAATGGA ATGCTTG-5'; miRNA mimics sense strand, 5'-CGUGAU UGCGAGACUCUGAdTdT-3' and antisense strand, 3'-dTdT GGCACUACGCUCUGAGACU-5'). A549 cells (1 $\times$ 10<sup>6</sup>) were transfected with 100 pmol plentivirus-si-MTA2 or plentivirus-siRNA-control at 25°C for 48 h (Ambion; Thermo Fisher Scientific, Inc.) using the Cell Line Nucleofector kit L and a Nucleofector I electroporation device according to a prewritten program (both from Lonza Group, Ltd.). All procedures were performed according to the manufacturer's instructions. The efficiency was determined by RT-qPCR (data not shown) as described below.

**Transfection of pMTA2.** A549 cells (1 $\times$ 10<sup>6</sup>) were cultured MEM with 5% FBS in six-well plate until 90% confluence. The media was subsequently removed. The MTA2 gene (GenBank, Y14808.1) was synthesized and cloned into pCMVp-NEO-X system (Takara Biotechnology Co., Ltd., Dalian, China). The recombinant vector was named pCMVp-NEO-MTA2 (pMTA2). Cells were transfected by pCMVp-NEO-MTA2 (2  $\mu$ g) using Lipofectamine 2000 (Sigma-Aldrich; Merck KGaA, Darmstadt, Germany), according to the manufacturer's instructions. Following 72 h transfection, subsequent experimentations were performed.

**ELISA analysis.** The affinity of the antibody against (Ab) MTA2 (cat. no. ab8106; Abcam, Cambridge, UK) with MTA2 was analyzed using an MTA2 commercial ELISA kit (cat. no. M7569-200UL; Thermo Fisher Scientific, Inc.), according to manufacturer's instructions. Briefly, A549 cells (1 $\times$ 10<sup>3</sup>) were cultured in 96-well plates (Invitrogen; Thermo Fisher Scientific, Inc.) pre-coated overnight at 4°C with AbMTA2, blocked with 1% bovine serum albumin (BSA; Sigma-Aldrich; Merck KGaA) in PBS for 1 h at 4°C, and incubated with standard MTA2 dilutions for 2 h at 37°C. Subsequently, AbMTA2 for 30 min at 37°C followed by washes with PBS

three times. The results were measured using an ELISA reader (Bio-Rad Laboratories, Inc., Hercules, CA, USA) reader at a wavelength of 450 nm.

**Reverse transcription-quantitative polymerase chain reaction (RT-qPCR).** Total RNA was extracted from A549 cells ( $1 \times 10^8$ ) pre- or post-treatment with AbMTA2 (5 mg/ml,  $1 \times 10^8$ ), siMTA2 transfection ( $1 \times 10^8$ ) or pMTA2 transfection ( $1 \times 10^8$ ) using an RNAeasy Mini kit (Qiagen Sciences, Inc., Gaithersburg, MD, USA) according to the manufacturer's instructions. Total RNA (1  $\mu$ g) was reverse transcribed into cDNA using the Reverse Transcription kit (Qiagen Sciences, Inc.) and the quality was confirmed using 1.5% agarose (Sigma-Aldrich; Merck KGaA) electrophoresis. cDNA (10 ng) was subjected to qPCR analysis with SYBR Green Master Mix system (Bio-Rad Laboratories, Inc.), according to the manufacturer's instructions. All the forward and reverse primers were synthesized by Invitrogen; Thermo Fisher Scientific, Inc. (Table I). Cycling conditions were as follows: 45 cycles of denaturation at 95°C for 2 min, annealing at 66°C for 30 sec with touchdown to 56°C for 30 sec, and extension at 72°C for 10 min. Relative mRNA expression changes were calculated using the  $2^{-\Delta\Delta C_q}$  method (42). Experiments were repeated three times and the results are expressed as the n-fold change relative to the control.

**MTT assay.** A549, pMTA2-, or siMTA2-transfected cells ( $1 \times 10^3$  cells/well) were incubated with AbMTA2 in 96-well plates for 72 h at 37°C in triplicate for each condition. At each time-point, 20  $\mu$ l MTT (5 mg/ml) in PBS solution was added to each well and the plate was further incubated for 4 h at 37°C. The medium was removed and 100  $\mu$ l dimethyl sulfoxide was added to the wells to solubilize the crystals. The optical density was measured using an ELISA microplate reader (Bio-Rad Laboratories, Inc.) at 450 nm.

**Induction of apoptosis in A549 cells.** A549, pMTA2-, siMTA2-transfected or AbMTA2-treated cells ( $1 \times 10^6$ ) were cultured in six-well plates until 80% confluence was reached. Apoptosis was assessed by incubating the cells with chemotherapeutic agent Taxol® (5 mg/ml) or PBS for 72 h at 37°C. Following incubation with AbMTA2, the cells were trypsinized and harvested by centrifuging at 2,000  $\times$  g for 10 min at room temperature. The cells were washed in cold PBS, adjusted to  $1 \times 10^6$  cells/ml with PBS, labeled with Annexin V-fluorescein isothiocyanate (FITC)/propidium iodide (Annexin V-FITC kit; BD Biosciences, Franklin Lakes, NJ, USA), and analyzed using a FACScan flow cytometer (BD Biosciences) and FlowJo 10.0.7 software (Tree Star, Inc., Ashland, OR, USA).

**Cell invasion and migration assays.** A549, pMTA2-, siMTA2-transfected, AbMTA2-treated or PBS-treated cells were seeded into the upper chamber of each insert. Subsequently, 500  $\mu$ l DMEM containing 10% FBS was added to a 24-well plate for 24 h. Migration and invasion analysis of cells was conducted in a 24-well culture plate with chamber inserts (BD Biosciences). For the migration assays,  $1 \times 10^4$  cells/well were placed into the upper chamber with a non-coated membrane. For the invasion assays, cells ( $5 \times 10^4$  cells/well) were placed into the upper chamber with a

Matrigel-coated membrane. All procedures were performed according to the manufacturer's instructions. The cells were fixed and stained for 30 min in a 0.1% crystal violet solution in PBS. The tumor cell invasion and migration was counted in at least three random fields/membrane, by light microscopy (Olympus Corporation, Tokyo, Japan) at  $\times 40$  magnification.

**Western blot analysis.** A549 cells ( $1 \times 10^7$ ) were treated with AbMTA2 (40 ng/ml) for 72 h. The A549 cells were harvested by scraping and lysed in radioimmunoprecipitation assay buffer (Invitrogen; Thermo Fisher Scientific, Inc.) followed by homogenization at 4°C for 10 min. Protein concentration was measured with a bicinchoninic acid protein assay kit (Thermo Fisher Scientific, Inc.). Proteins (10  $\mu$ g) were analyzed by 15% SDS-PAGE and transferred onto polyvinylidene fluoride membranes (EMD Millipore, Billerica, MA, USA). Membranes were blocked with 5% BSA (Sigma-Aldrich; Merck KGaA) for 2 h at room temperature and probed with antibodies (Abcam) against the following proteins: MTA2 (1:1,000; cat. no. ab5392), ERK (1:1,000; cat. no. ab17942), AKT (1:1,000; cat. no. ab8805), matrix metalloproteinase 2 (1:5,000; MMP2; cat. no. ab7033), MMP-9 (cat. no. ab38898), cardiotrophin-1 (CT-1; cat. no. ab80527), tRNA 2'-O-methyltransferase fibronectin (FIB; 1:1,000; cat. no. ab2413), E-cadherin (1:1,000; cat. no. ab76055), Snail (1:1,000; cat. no. ab53519), caspase-3 (1:2,000; cat. no. ab13585), Bcl2-associated agonist of cell death (Bad; 1:1,000; cat. no. ab32060), N-cadherin (1:2,000; cat. no. ab18203), p-ERK (1:2,000; cat. no. ab192591), pAKT (1:2,000; cat. no. ab81283), vimentin (1:1,000; cat. no. ab92547) and  $\beta$ -actin (1:2,000; cat. no. ab8827) for 12 h at 4°C. The horseradish peroxidase-conjugated anti-rabbit IgG secondary antibody (cat. no. VPA00764; Bio-Rad Laboratories, Inc.) was used at a 1:5,000 dilution for 2 h at 4°C and detected using enhanced chemiluminescence substrate ECL Select™ (GE Healthcare Life Sciences, Little Chalfont, UK), according to the manufacturer's instructions. The density of the bands was analyzed using Quantity One software version 4.62 (Bio-Rad Laboratories, Inc.).

**Immunofluorescence.** A549 cells ( $1 \times 10^6$ ) were cultured in six-well plates until a 90% confluent monolayer was achieved. The cells were subsequently incubated with a mouse anti-human MTA2 primary antibody (1:1,000; cat. no. ab5392; Abcam) for 12 h at 4°C. The cells were washed with PBS to completely remove the residual antibody and incubated with horseradish peroxidase-conjugated anti-rabbit IgG secondary antibody (1:5,000; cat. no. 1721019; Bio-Rad Laboratories, Inc.) for 2 h at 37°C. Following washing in PBS, cells were mounted with anti-fade reagent DAPI (Invitrogen; Thermo Fisher Scientific, Inc.) for 2 h at 37°C and viewed with fluorescent microscope (Olympus Corporation, Tokyo, Japan) at  $\times 40$  magnification.

**Immunohistochemistry.** Tumors from NSCLC carcinoma xenograph mice treated with AbMTA2 or PBS were excised on day 30 and fixed using 10% formaldehyde followed by embedding in paraffin wax, and cut into serial sections (4  $\mu$ m). Tissues were washed with PBS-Tween-20 (PBST) three times at room temperature and antigen retrieval was



Table I. Sequences of primers.

| Gene name      | Sequence                                   |                                       |
|----------------|--|---------------------------------------|
|                | Reverse                                    | Forward                               |
| VEGFR1         | 5'-TCACTGCCACTCTAATTGTC-3'                 | 5'-CCATATGCGGTACAAGTCA-3'             |
| VEGFR2         | 5'-AAGGCGAGACCTGCATTC-3'                   | 5'-CTGCCCTCTTCTGAGCTCT-3'             |
| VEGFR3         | 5'-AGCCATTCATCAACAAGCCT-3'                 | 5'-GGCAACAGCTGGATGTCATA-3'            |
| VEGF           | 5'-TGCATTCACATTGTGCTGCTGTAG-3'             | 5'-GCAGATTATGCGGATCAAACC-3'           |
| EGF            | 5'-CATCCAGTGAGACCAATGAG-3'                 | 5'-GTAGCCGCCAGTTCACCATT-3'            |
| Ep-CAM         | 5'-TGCTGAACTGAAGTACACTGGCAT<br>TGGTTTTG-3' | 5'-CCTGAACTGAAGTACTGGCATTGGTCACTCA-3' |
| TAF            | 5'-ACTGGCAGTATGTGCACTGC-3'                 | 5'-CAGCCTGGGTCAGGGTCAATCCCT-3'        |
| $\beta$ -actin | 5'-CATCTCTTGCTCGAAGTCCA-3'                 | 5'-ATCATGTTTGAGACCTTCAACA-3'          |

VEGF, vascular endothelial growth factor; Ep-CAM, epithelial cell adhesion molecule; TAF, tumor angiogenesis factor; EGF, pro-epidermal growth factor.

performed on the tumor sections using a microwave heating AR (43) subsequent to a series of ethanols (100, 95 and 80%). Tumor sections were washed with PBST at room temperature and incubated with primary antibodies: EGF (1:500; cat. no. ab9695), and VEGF (1:500; cat. no. ab32152) (both from Abcam) at 37°C for 2 h. Then, sections were blocked with 5% BSA (Sigma-Aldrich; Merck KGaA) at 37°C for 2 h and horseradish peroxidase-conjugated anti-rabbit IgG secondary antibody (Bio-Rad Laboratories, Inc.) was used to incubate primary antibodies at a 1:5,000 dilution at 37°C for 2 h. A Ventana Benchmark Automated Staining System (Ventana Medical Systems, Inc., Tucson, AZ, USA) was used for the observation of protein expression.

**Animal study.** A total of 80 specific pathogen-free female nude mice (age, 6 weeks; body weight, 30–36 g) were purchased from Shanghai SLAC Laboratory Animal Co., Ltd. (Shanghai, China). All animals were given free access to food and water and housed in a temperature-controlled facility at 23±1°C and relative humidity of 50±5% with a 12-h light/dark cycle. Mice were subcutaneously implanted with MTA2-overexpression (n=20), MTA2-silenced (n=20) or A549 tumor cells (1×10<sup>6</sup> cells) (n=20), AbMTA2 (n=20). The A549 group was divided into two groups (n=20/group) and received intravenously injected AbMTA2 (500 ng/kg) or PBS (500 ng/kg). Treatments began on day 7 following tumor cell implantation, when the tumor diameter reached 5–7 mm. The treatment was continued for 7 days at a frequency of once per day. The tumor volumes were calculated according to a previous study (44). Animals (n=15 in each group) were housed for 120 days to investigate the role of MTA2 in NSCLC.

**Statistical methods.** All data are presented as the mean ± standard error of the mean of triplicate experiments, and were analyzed using GraphPad Prism version 5.0 software (GraphPad Software, Inc., La Jolla, CA, USA). Unpaired data were analyzed using Student's t-test and comparisons of data between multiple groups were performed using one-way

analysis of variance followed by Whitney rank test or Fisher's exact test. The Kaplan-Meier test was used to estimate the risk of relapse and re-treatment during a 120-day treatment. P<0.05 was considered to indicate a statistically significant difference.

## Results

**MTA2 expression and its function in NSCLC cells.** A comparison of the levels of expression revealed that the MTA2 protein was expressed at notably higher levels in two NSCLC cell lines, A549 and H358, compared with a normal lung cell line, MRC-5 (Fig. 1A). To analyze the function of MTA2 in NSCLC cells, A549 cell cultures were established by transfection with MTA2 overexpression plasmids (pMTA2) or lentivirus-mediated siRNA-MTA2. MTA2 expression was increased following transfection with pMTA2, and decreased following si-MTA2 transfection (Fig. 1B). It was observed that MTA2 overexpression resulted in a significant increase in A549 cell growth, whereas si-MTA2 transfection inhibited NSCLC growth (Fig. 1C). Migration and invasion assays demonstrated that MTA2 is positively associated with aggressiveness (Fig. 1D and E) MTA2 downregulation inhibited migration and invasion of NSCLC cells, while MTA2 overexpression promoted migration and invasion of NSCLC cells. The apoptosis assay demonstrated that pMTA2 decreased the apoptosis of A549 cells induced by the chemotherapeutic agent Taxol<sup>®</sup> compared to control (Fig. 1F). The results of the present study indicated that MTA2 proteins are more highly expressed in NSCLC cells and may be positively associated with growth, aggressiveness and apoptotic resistance of NSCLC cells.

**AbMTA2 suppresses MTA2-induced aggressiveness in NSCLC cells.** The efficacy of AbMTA2 was assessed in NSCLC cells, which indicated that AbMTA2 was able to specifically bind to MTA2, as determined by ELISA analysis (Fig. 2A). Immunofluorescence and western blotting experiments demonstrated that AbMTA2 efficiently

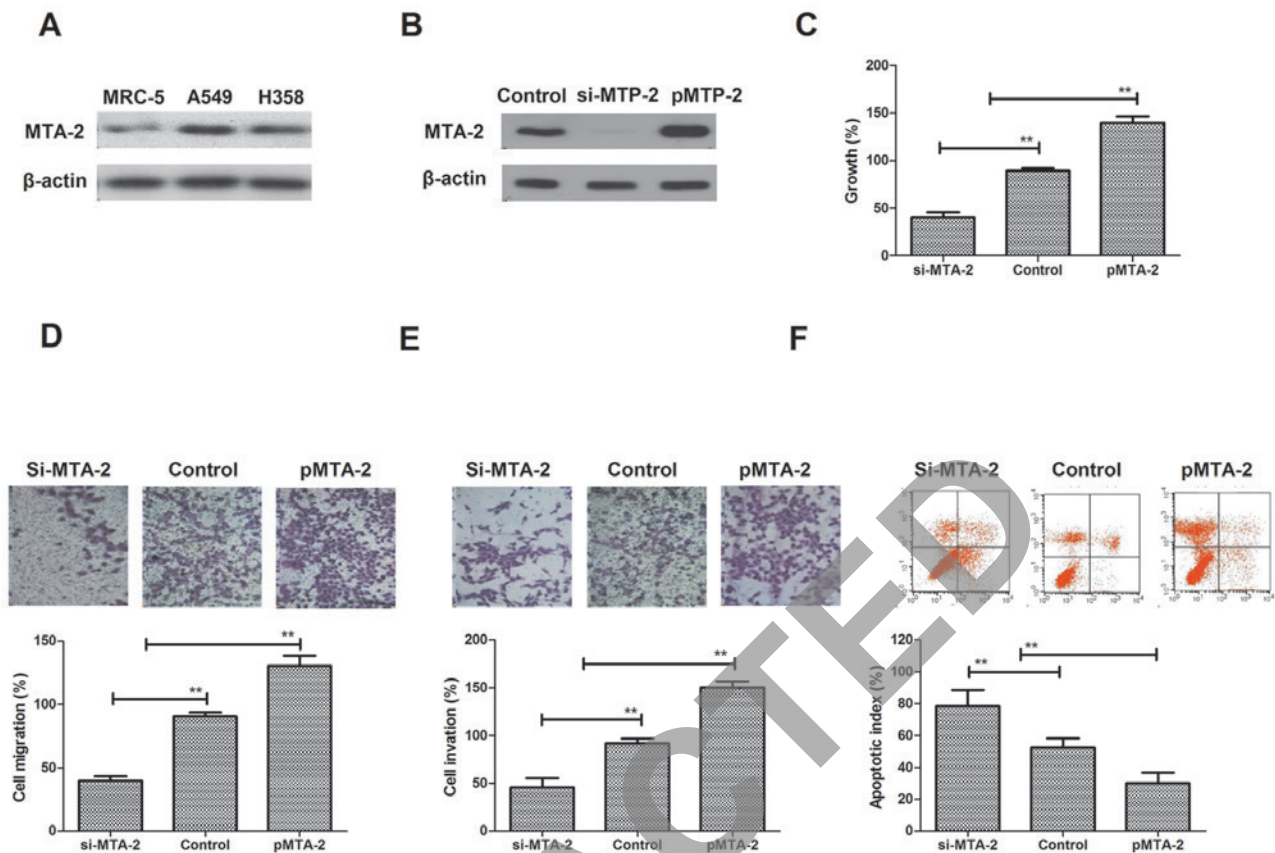


Figure 1. MTA2 expression and regulatory effects on NSCLC cells. (A) MTA2 expression in NSCLC and normal human lung cells. (B) Detection of MTA2 expression in lentivirus-mediated si-MTA2 and MTA2 overexpression NSCLC cells. (C) Analysis of the association between MTA2 and the growth of NSCLC cells. (D) Analysis of the association between MTA2 and the migration of NSCLC cells. Magnification,  $\times 400$ . (E) Analysis of the association between MTA2 and the invasion of NSCLC cells. Magnification,  $\times 400$ . (F) Apoptosis rate of A549 cells in conditions of MTA2 overexpression and loss. The data are presented as the mean  $\pm$  standard error of the mean of three independent experiments. \*\* $P < 0.01$  vs. control. MTA2, metastasis associated protein MTA2; NSCLC, non-small cell lung carcinoma; si, small interfering.

suppressed MTA2 protein expression in A549 cells (Fig. 2B). In addition, AbMTA2-suppressed expression cells exhibited decreased expression of MTA2 target genes, including MMP-2, MMP-9, CT-I and FIB compared with untransfected control cells (Fig. 2C). In addition, migration and invasion assays demonstrated that AbMTA2 markedly inhibited the aggressiveness of A549 cells (Fig. 2D and E). Furthermore, apoptotic resistance was inhibited in A549 cells following treatment with AbMTA2 for 48 h (Fig. 2F). The results of the present study indicated that AbMTA2 may be a potential agent for the inhibition of migration and invasion in NSCLC cells.

**MTA2 regulates migration and invasion of NSCLC cells via the ERK/AKT and VEGF signaling pathways.** To analyze the mechanisms underlying MTA2-mediated growth and metastasis in NSCLC cells, the ERK/AKT and VEGF signaling pathways were analyzed. The protein expression levels of E-cadherin, Snail, N-cadherin and Vimentin were analyzed, and it was observed that AbMTA2 markedly inhibited the expression of these proteins in A549 cells (Fig. 3A). To confirm that AbMTA2 inhibited the epithelial-mesenchymal transition process via the ERK/AKT signaling pathway, the protein expression levels of ERK and AKT were analyzed. The data demonstrated that pMTA2 increased, while si-MTA2

and AbMTA2 suppressed ERK and AKT expression in A549 cells compared with untreated control cells (Fig. 3B). The expression levels of apoptosis-associated proteins Caspase-3 and Bad also exhibited a decreased expression following treatment with AbMTA2 and si-MTA2 (Fig. 3C). However, pMTA2 increased the expression of caspase-3 and Bad in A549 cells.

It was also demonstrated that VEGF and EGF mRNA expression levels were decreased following treatment with AbMTA2 and si-MTA2 in A549 cells (Fig. 3E). AbMTA2 and si-MTA2 resulted in the decreased mRNA expression of Ep-CAM and tumor angiogenesis factor in A549 cells, while pMTA2 exerted the reverse effect (Fig. 3F). The present results demonstrated that si-MTA2 exerted similar effects on inhibition of ERK/AKT and VEGF signaling pathways in NSCLC cells, while pMTA2 promoted ERK/AKT and VEGF signaling pathways in NSCLC cells. The results of the present study demonstrated that MTA2 regulated the expression of components of the ERK/AKT and VEGF signaling pathways in A549 cells *in vitro*.

***In vivo* inhibitory effects of AbMTA2 on A549-bearing mice.** To investigate whether the inhibition of MTA2 protein expression was able to inhibit NSCLC growth *in vivo*, NSCLC-bearing mice were established for further analysis.

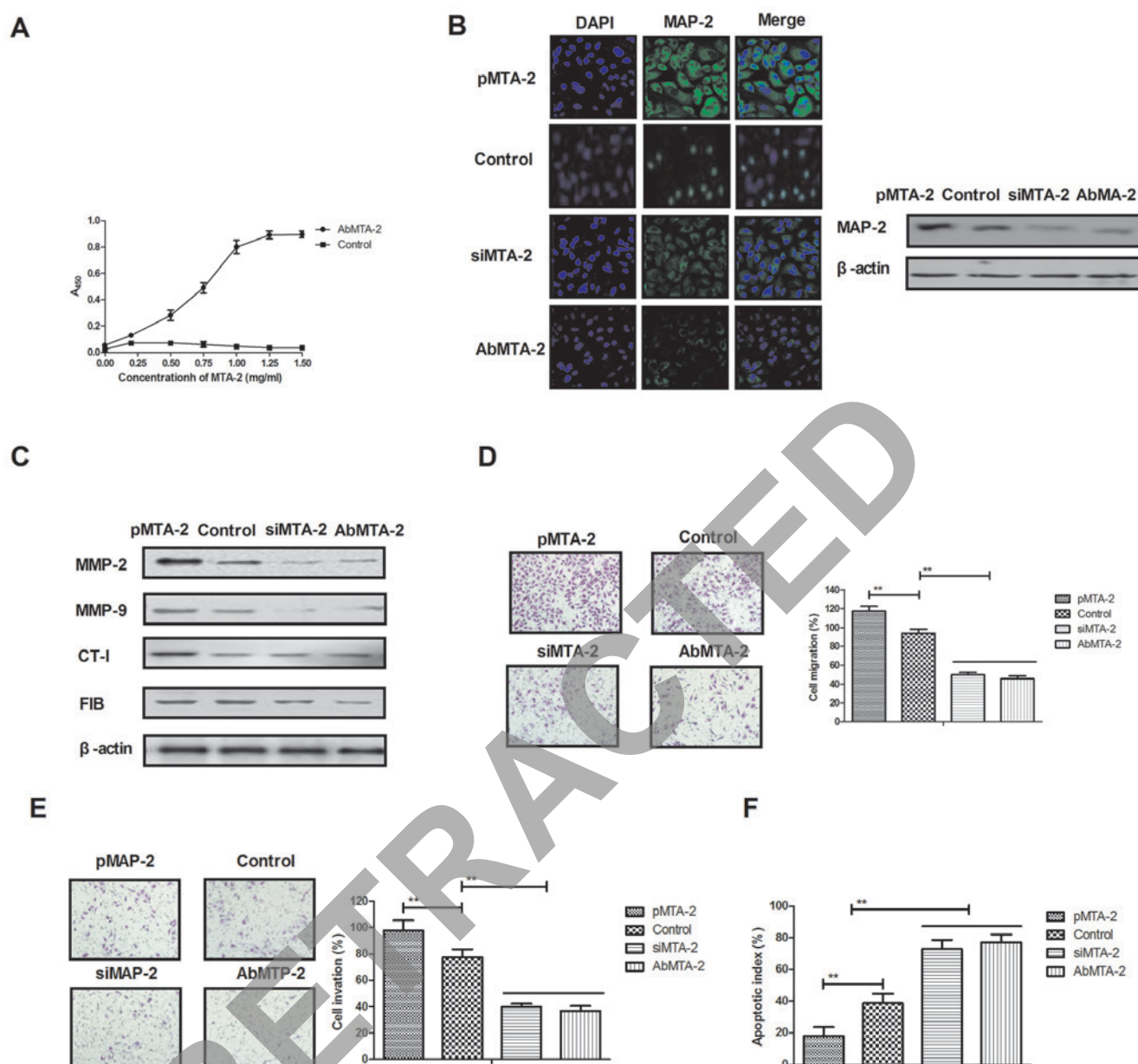


Figure 2. Targeting MTA2 suppresses the growth and aggressiveness of non-small cell lung carcinoma cells. (A) Affinity of AbMTA2 with MTA2 as determined by ELISA analysis. (B) Immunofluorescence and western blotting experiments analyzed the efficiency of AbMTA2 targeting for MTA. Magnification, x200. (C) Expression of MTA2 target genes in A549 cells. (D) Migration of A549 cells following treatment with AbMTA2. Magnification, x400. (E) Invasion of A549 cells following treatment with AbMTA2. Magnification, x400. (F) Apoptotic resistance of A549 cells following treatment with AbMTA2. The data are presented as the mean  $\pm$  standard error of the mean of three independent experiments. \*\* $P < 0.01$ . MTA2, metastasis associated protein MTA2; siRNA, small interfering RNA; MMP-2, 72 kDa type IV collagenase; MMP-9, matrix metalloproteinase-9; CT-1, cardiotrophin-1; FIB, rRNA 2'-O-methyltransferase fibrillarin; Ab, antibody.

The antitumor efficacy of AbMTA2 was assessed in the NSCLC mouse model. The results in Fig. 4A demonstrated that tumor size was significantly inhibited in A549-bearing nude mice following AbMTA2 treatment, compared with mice treated with PBS, si-MTA2 transfection and pMTA2 transfection ( $P < 0.01$ ), whereas MTA2-overexpressing cells developed a large tumor mass. We demonstrated that si-MTA2 transfection significantly inhibited tumor growth compared to pMTA2 transfection and PBS-treated mice ( $P < 0.01$ ). Immunohistochemistry and western blotting results of the present study indicated that ERK and AKT protein expressions were decreased following treatment with AbMTA2 and si-MTA2 transfection compared with pMTA2 transfection

and PBS-treated mice (Fig. 4B). In addition, it was observed that VEGF protein expression was reduced in AbMTA2 and si-MTA2 transfection groups compared to pMTA2 transfection and PBS-treated groups (Fig. 4C). Additionally, long-term (120-day observation) survival analysis demonstrated that AbMTA2 therapy and si-MTA2 transfection significantly prolonged the survival of NSCLC-bearing mice compared with pMTA2 transfection and PBS-treated groups (Fig. 4D;  $n = 12/\text{group}$ ). The results of the present study indicated that treatment with AbMTA2 significantly decreased ERK, AKT and VEGF protein expression levels, which may translate into long-term survival and tumor-free living in A549-bearing mice.



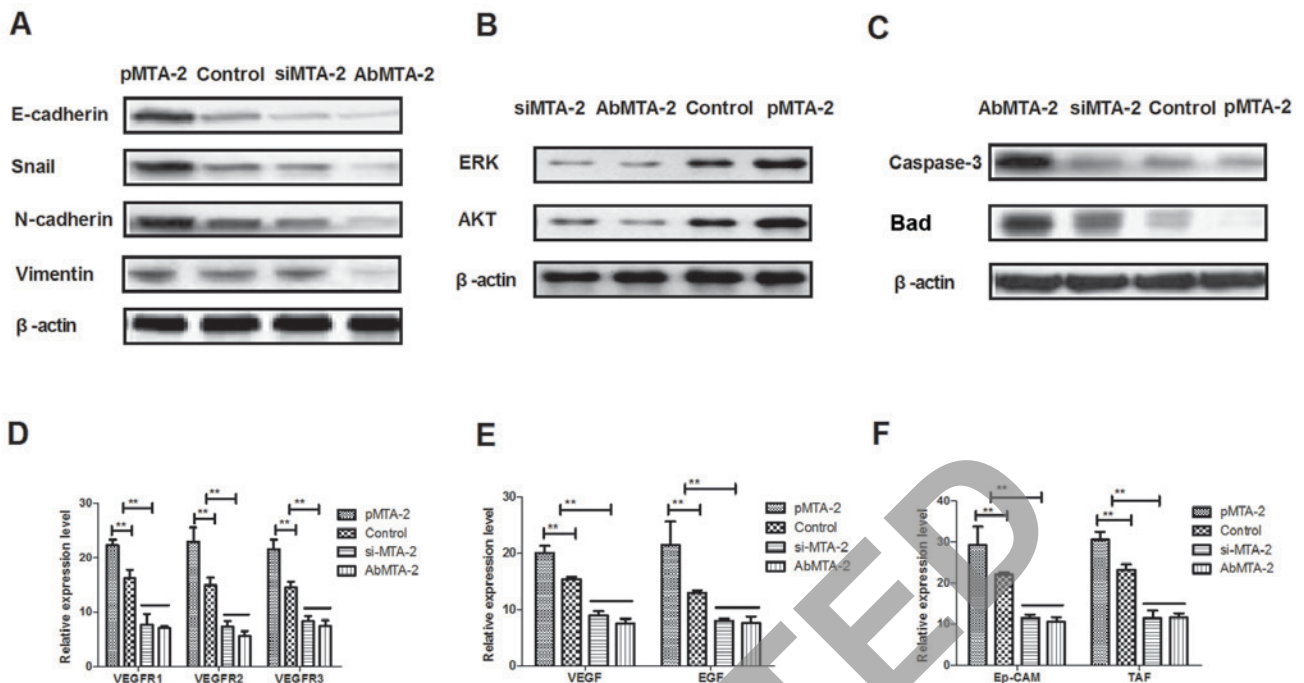


Figure 3. Mechanism of MTA2-mediated signaling pathways in non-small cell lung carcinoma cells. (A) E-cadherin, Snail, N-cadherin and vimentin expression levels in A549 cells following treatment with the indicated agents. (B) ERK and AKT expression in A549 cells following treatment with the indicated agents. (C) Apoptosis-associated proteins caspase-3 and Bad expression levels in A549 cells. (D) VEGFR1, VEGFR2 and VEGFR3 expression levels in AbMTA2-treated A549 cells. (E) VEGF and EGF expression levels in AbMTA2-treated A549 cells. (F) Ep-CAM and TAF expression in A549 cells. The data are presented as the mean  $\pm$  standard error of the mean of three independent experiments. \*\* $P < 0.01$  vs. control. MTA2, metastasis associated protein MTA2; Snail, zinc-finger protein SNAI1; ERK, extracellular signal-regulated kinase; AKT, RAC- $\alpha$  serine/threonine protein kinase; Bad, Bcl2-associated agonist of cell death; VEGFR, vascular endothelial growth factor receptor; EGF, pro-epidermal growth factor; Ep-CAM, epithelial cell adhesion molecule; TAF, tumor angiogenesis factor; si, small interfering; Ab, antibody.

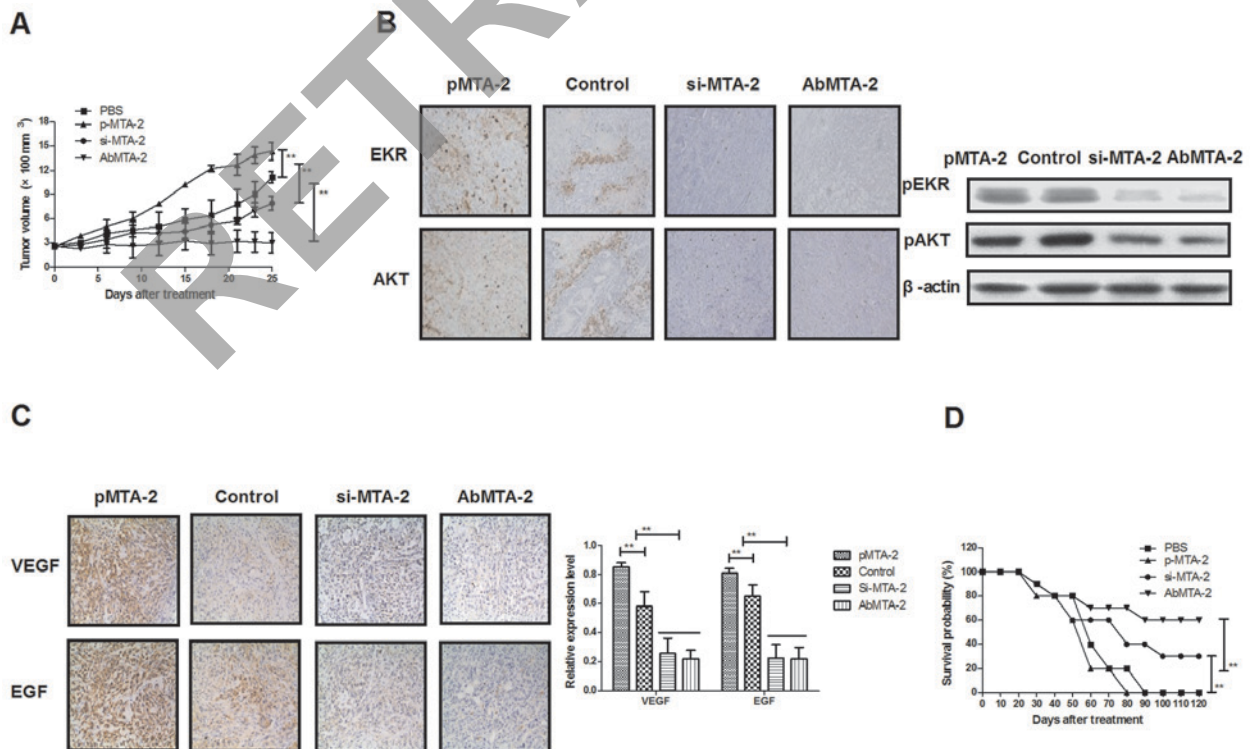


Figure 4. Therapeutic effects of AbMTA2 on A549-bearing mice *in vivo*. (A) Growth of non-small cell lung carcinoma tumor in A549-bearing mice following treatment with the indicated agents. (B) ERK and AKT expression levels in the experimental tumor on day 25. Magnification, x400. (C) VEGF and EGF expression levels in the experimental tumor on day 25. Magnification, x400. (D) Long-term (120-day observation) survival of A549-bearing mice following treatment with the indicated agents. The data are presented as the mean  $\pm$  standard error of the mean of three independent experiments. \*\* $P < 0.01$  vs. control. Ab, antibody; MTA2, metastasis associated protein MTA2; ERK, extracellular signal-regulated kinase; AKT, RAC- $\alpha$  serine/threonine protein kinase; VEGF, vascular endothelial growth factor; EGF, pro-epidermal growth factor; si, small interfering.

## Discussion

The occurrence of lung cancer has been associated with industrial pollution and destruction of the ecological environment in developed countries (45). Although a number of clinical treatments have been proposed, these strategies frequently lead to toxic side effects and are ineffective (46). Molecular-targeted therapies have the potential to be highly targeted alternatives, with decreased toxicity to normal human tissues and with the capacity to completely eradicate the tumor (47-49). These therapies work by using multi-targeted therapeutic drugs that are able to directly target antigens on malignant cells. To date, a number of molecular-targeted therapies have been demonstrated to be successful in treating human lung cancer (50). A previous study demonstrated that MTA2 may serve an important role in tumor progression, and may be a potential target for human cancer therapy (51). In the present study, a targeted therapy antibody towards MTA2 was constructed for the treatment of human NSCLC, and its efficacy was investigated in NSCLC cells and xenograft mice. The results demonstrated that antibody targeting of MTA2 may be an efficient strategy for the treatment of NSCLC.

NSCLC is the main type of human lung cancer (>80% of lung cancer cases) and is frequently diagnosed at an advanced stage. Therefore, the majority of patients with NSCLC exhibit a limited survival rate post-diagnosis (52). In addition, the relatively higher rates of morbidity and mortality of NSCLC, compared with other types of human cancer, have become an issue of increasing importance (53). A previous study reported that the number of cases of NSCLC has been increasing in recent years, which has become a public health focus (54). Therefore, understanding the pathogenesis of NSCLC and the mechanisms of its progression is required for the development of treatments for NSCLC.

A number of signaling pathways have been suggested to be involved in NSCLC progression, and have been targets of clinical and literature research. It was hypothesized that NSCLC may become resistant to therapies through feedback mechanisms that may compensate for targeted inhibition (55). Molecular targets of the VEGF and ERK/AKT pathways may simultaneously inhibit two important signaling pathways activated in NSCLC cells and may overcome one potential aspect of resistance to single-agent therapy. Previous studies have suggested that treatment options may be available for targeting the VEGF and ERK/AKT-mediated pathways (56,57). In the present study, the MTA2-mediated mechanism in NSCLC cells was analyzed to elucidate the role of signaling pathways following treatment with AbMTA2. The results indicated that MTA2 may regulate the growth and aggressiveness of NSCLC via the ERK/AKT and VEGF signaling pathways. Notably, it was identified that AbMTA2 treatment decreased the apoptotic resistance of NSCLC cells induced by chemotherapy with Taxol®. Treatment with AbMTA2 inhibited growth through the VEGF signaling pathway and suppressed migration and invasion via the ERK/AKT signaling pathway.

The present study identified AbMTA2 to be an efficient anti-NSCLC agent for the inhibition of development and metastasis, which has been reported to be associated with NSCLC cell proliferation, migration and invasion (58). The

results of the present study demonstrated that AbMTA2 regulated proliferation, migration and invasion through the ERK/AKT and VEGF signaling pathways in tumor cells and xenograft models. Notably, it was additionally observed that AbMTA2 decreased apoptotic resistance via downregulation of caspase-3 and Bad expression in NSCLC cells. The results of the present study suggested that MTA2 may be a potential target in NSCLC and that AbMTA2 may be able to inhibit NSCLC proliferation and invasion through inhibition of the ERK/AKT and VEGF signaling pathways.

## References

- Magnuson WJ, Yeung JT, Guillod PD, Gettinger SN, Yu JB and Chiang VL: Impact of deferring radiation therapy in patients with epidermal growth factor receptor-mutant non-small cell lung cancer who develop brain metastases. *Int J Radiat Oncol Biol Phys* 95: 673-679, 2016.
- Fenton-Ambrose L and Kazerooni EA: Preventative care: Lung-cancer screens now worth the cost. *Nature* 514: 35, 2014.
- Zhukovsky M, Varaksin A and Pakholkina O: Statistical analysis of observational study of the influence of radon and other risk factors on lung cancer incidence. *Radiat Prot Dosimetry* 160: 108-111, 2014.
- Brody H: Lung cancer. *Nature* 513: S1, 2014.
- Moro-Sibilot D, Smit E, de Castro Carpeno J, Lesniewski-Kmak K, Aerts JG, Villatoro R, Kraaij K, Nacerddine K, Dyachkova Y, Smith KT, *et al*: Non-small cell lung cancer patients with brain metastases treated with first-line platinum-doublet chemotherapy: Analysis from the European FRAME study. *Lung Cancer* 90: 427-432, 2015.
- Barnett SA, Downey RJ, Zheng J, Plourde G, Shen R, Chaff J, Akhurst T, Park BJ and Rusch VW: Utility of routine pet imaging to predict response and survival after induction therapy for non-small cell lung cancer. *Ann Thorac Surg* 101: 1052-1059, 2016.
- Jiang SY, Zhao J, Wang MZ, Huo Z, Zhang J, Zhong W and Xu Y: Small-cell lung cancer transformation in patients with pulmonary adenocarcinoma: A case report and review of literature. *Medicine (Baltimore)* 95: e2752, 2016.
- Kong R, Feng J, Ma Y, Zhou B, Li S, Zhang W, Jiang J, Zhang J, Qiao Z, Zhang T, *et al*: Silencing NACK by siRNA inhibits tumorigenesis in non-small cell lung cancer via targeting Notch1 signaling pathway. *Oncol Rep* 35: 2306-2314, 2016.
- Bablekos GD, Analitis A, Michaelides SA, Charalabopoulos KA and Tzonou A: Management and postoperative outcome in primary lung cancer and heart disease co-morbidity: A systematic review and meta-analysis. *Ann Transl Med* 4: 213, 2016.
- Liu Y, Ren Z, Wang J and Zhang S: Epidermal growth factor receptor-tyrosine kinase inhibitor therapy is especially beneficial to patients with exon 19 deletion compared with exon 21 L858R mutation in non-small-cell lung cancer: Systematic review and meta analysis. *Thorac Cancer* 7: 406-414, 2016.
- Abar L, Vieira AR, Aune D, Stevens C, Vingeliene S, Navarro Rosenblatt DA, Chan D, Greenwood DC and Norat T: Blood concentrations of carotenoids and retinol and lung cancer risk: An update of the WCRF-AICR systematic review of published prospective studies. *Cancer Med* 5: 2069-2083, 2016.
- Xie FJ, Lu HY, Zheng QQ, Qin J, Gao Y, Zhang YP, Hu X and Mao WM: The clinical pathological characteristics and prognosis of FGFR1 gene amplification in non-small-cell lung cancer: A meta-analysis. *Onco Targets Ther* 9: 171-181, 2016.
- Lim SH, Sun JM, Lee SH, Ahn JS, Park K and Ahn MJ: Pembrolizumab for the treatment of non-small cell lung cancer. *Expert Opin Biol Ther* 16: 397-406, 2016.
- Kular H, Mudambi L, Lazarus DR, Cornwell L, Zhu A and Casal RF: Safety and feasibility of prolonged bronchoscopy involving diagnosis of lung cancer, systematic nodal staging, and fiducial marker placement in a high-risk population. *J Thorac Dis* 8: 1132-1138, 2016.
- Nakagawa K, Asamura H, Tsuta K, Nagai K, Yamada E, Ishii G, Mitsudomi T, Ito A, Higashiyama M, Tomita Y, *et al*: The novel one-step nucleic acid amplification (OSNA) assay for the diagnosis of lymph node metastasis in patients with non-small cell lung cancer (NSCLC): Results of a multicenter prospective study. *Lung Cancer* 97: 1-7, 2016.



16. Müller B, Bovet M, Yin Y, Stichel D, Malz M, González-Vallinas M, Middleton A, Ehemann V, Schmitt J, Muley T, *et al*: Concomitant expression of far upstream element (FUSE) binding protein (FBP) interacting repressor (FIR) and its splice variants induce migration and invasion of non-small cell lung cancer (NSCLC) cells. *J Pathol* 237: 390-401, 2015.
17. Zhao Q, Yue J, Zhang C, Gu X, Chen H and Xu L: Inactivation of M2 AChR/NF- $\kappa$ B signaling axis reverses epithelial-mesenchymal transition (EMT) and suppresses migration and invasion in non-small cell lung cancer (NSCLC). *Oncotarget* 6: 29335-29346, 2015.
18. Zhang H, Zhu X, Li N, Li D, Sha Z, Zheng X and Wang H: miR-125a-3p targets MTA1 to suppress NSCLC cell proliferation, migration, and invasion. *Acta Biochim Biophys Sin (Shanghai)* 47: 496-503, 2015.
19. Roth MT, Ivey JL, Esserman DA, Crisp G, Kurz J and Weinberger M: Individualized medication assessment and planning: Optimizing medication use in older adults in the primary care setting. *Pharmacotherapy* 33: 787-797, 2013.
20. Ibrahim M, Parry S, Wilkinson D, Bilbe N, Allen D, Forrest S, Maxwell P, O'Grady A, Starczynski J, Tanier P, *et al*: ALK immunohistochemistry in non-small cell lung carcinoma (NSCLC): Discordant staining can impact patient treatment regimen. *J Thorac Oncol* 11: 2241-2247, 2016.
21. Cadranet J, Park K, Arrieta O, Pless M, Bendaly E, Patel D, Sasane M, Nosal A, Swallow E, Galebach P, *et al*: Characteristics, treatment patterns, and survival among ALK<sup>+</sup> non-small cell lung cancer (NSCLC) patients treated with crizotinib: A chart review study. *Lung Cancer* 98: 9-14, 2016.
22. Passaro A, Spitaleri G and de Marinis F: First-line treatment in NSCLC harboring EGFR common mutations: EGFR TKI in monotherapy or in combination with anti-VEGF? *Expert Rev Anticancer Ther* 16: 799-801, 2016.
23. Izuishi K and Mori H: Recent strategies for treating stage iv gastric cancer: Roles of palliative gastrectomy, chemotherapy, and radiotherapy. *J Gastrointest Liver Dis* 25: 87-94, 2016.
24. Hsieh CE, Lin CY, Lee LY, Yang LY, Wang CC, Wang HM, Chang JT, Fan KH, Liao CT, Yen TC, *et al*: Adding concurrent chemotherapy to postoperative radiotherapy improves locoregional control but not overall survival in patients with salivary gland adenoid cystic carcinoma-a propensity score matched study. *Radiat Oncol* 11: 47, 2016.
25. Khalil EM and Anwar MM: Treatment results of pediatric nasopharyngeal carcinoma, NCI, Cairo University experience. *J Egypt Natl Canc Inst* 27: 119-128, 2015.
26. Wang Y, Lan G, Si Y, Deng Z, Sun J, Yang Y, Han X, Weng J and Zhou F: Treatment and outcome of recurrent cervical lymph nodes in patients with nasopharyngeal carcinoma after radiotherapy. *Zhonghua Er Bi Yan Hou Tou Jing Wai Ke Za Zhi* 51: 183-188, 2016 (In Chinese).
27. Casanova M, Özyar E, Patte C, Orbach D, Ferrari A, Veyrat-Follet C, Errihani H, Pan J, Zhang L, Shen L, *et al*: International randomized phase 2 study on the addition of docetaxel to the combination of cisplatin and 5-fluorouracil in the induction treatment for nasopharyngeal carcinoma in children and adolescents. *Cancer Chemother Pharmacol* 77: 289-298, 2016.
28. Co J, Mejia MB and Dizon JM: Evidence on effectiveness of intensity-modulated radiotherapy versus 2-dimensional radiotherapy in the treatment of nasopharyngeal carcinoma: Meta-analysis and a systematic review of the literature. *Head Neck* 38 (Suppl 1): E2130-E2142, 2016.
29. Colaco RJ, Betts G, Donne A, Swindell R, Yap BK, Sykes AJ, Slevin NJ, Homer JJ and Lee LW: Nasopharyngeal carcinoma: A retrospective review of demographics, treatment and patient outcome in a single centre. *Clin Oncol (R Coll Radiol)* 25: 171-177, 2013.
30. Setton J, Wolden S, Caria N and Lee N: Definitive treatment of metastatic nasopharyngeal carcinoma: Report of 5 cases with review of literature. *Head Neck* 34: 753-757, 2012.
31. Caponigro F, Longo F, Ionna F and Perri F: Treatment approaches to nasopharyngeal carcinoma: A review. *Anticancer Drugs* 21: 471-477, 2010.
32. Marcy PY, Zhu Y and Bensadoun RJ: Target volumes in radiotherapy-head and neck tumors intensity-modulated radiation therapy (IMRT) of nasopharyngeal carcinoma: Practical aspects in the delineation of target volumes and organs at risk. *Cancer Radiother* 9: 240-250, 2005 (In French).
33. Li Y, Xie G and Pan Z: Advancement biological target therapy of nasopharyngeal carcinoma. *Lin Chung Er Bi Yan Hou Tou Jing Wai Ke Za Zhi* 29: 671-673, 2015 (In Chinese).
34. Miyashita T, Tajima H, Munemoto M, Shah FA, Harmon JW, Watanabe T, Shoji M, Okamoto K, Nakanuma S, Sakai S, *et al*: Impact of histone deacetylase 1 and metastasis-associated gene 1 expression in esophageal carcinogenesis. *Oncol Lett* 8: 758-764, 2014.
35. Lee MH, Na H, Na TY, Shin YK, Seong JK and Lee MO: Epigenetic control of metastasis-associated protein 1 gene expression by hepatitis B virus X protein during hepatocarcinogenesis. *Oncogenesis* 3: e88, 2014.
36. Wang Y, Jia H, Lin H, Tan X, Du Z, Chen H, Xu Y, Han X, Zhang J, Zhao S, *et al*: Metastasis-associated gene, mag-1 improves tumour microenvironmental adaptation and potentiates tumour metastasis. *J Cell Mol Med* 16: 3037-3051, 2012.
37. Reddy SD, Pakala SB, Molli PR, Sahni N, Karanam NK, Mudvari P and Kumar R: Metastasis-associated protein 1/histone deacetylase 4-nucleosome remodeling and deacetylase complex regulates phosphatase and tensin homolog gene expression and function. *J Biol Chem* 287: 27843-27850, 2012.
38. Fu J, Qin L, He T, Qin J, Hong J, Wong J, Liao L and Xu J: The TWIST/Mi2/NuRD protein complex and its essential role in cancer metastasis. *Cell Res* 21: 275-289, 2011.
39. Gururaj AE, Holm C, Landberg G and Kumar R: Breast cancer-amplified sequence 3, a target of metastasis-associated protein 1, contributes to tamoxifen resistance in premenopausal patients with breast cancer. *Cell Cycle* 5: 1407-1410, 2006.
40. Jia W, Zhu J, Martin TA, Sanders AJ, Yang X, Cheng S, Yu H, Jia G, Liu X, Lu R and Jiang WG: Expression of metastasis-associated gene-1 is associated with bone invasion and tumor stage in human pituitary adenomas. *Cancer Genomics Proteomics* 12: 113-118, 2015.
41. Zhang B, Zhang H and Shen G: Metastasis-associated protein 2 (MAP2) promotes the metastasis of non-small-cell lung cancer through the inhibition of the cell adhesion molecule Ep-CAM and E-cadherin. *Jpn J Clin Oncol* 46: 393, 2016.
42. Livak KJ and Schmittgen TD: Analysis of relative gene expression data using real-time quantitative PCR and the 2(-Delta Delta C(T)) method. *Methods* 25: 402-408, 2001.
43. Shi S, Zhang P, Cheng Q, Wu J, Cui J, Zheng Y, Bai XY and Chen X: Immunohistochemistry of deparaffinised sections using antigen retrieval with microwave combined pressure cooking versus immunofluorescence in the assessment of human renal biopsies. *J Clin Pathol* 66: 374-380, 2013.
44. Zhuang T, Djemil T, Qi P, Magnelli A, Stephans K, Videtic G and Xia P: Dose calculation differences between Monte Carlo and pencil beam depend on the tumor locations and volumes for lung stereotactic body radiation therapy. *J Appl Clin Med Phys* 14: 4011, 2013.
45. Lee YT, Liu CJ, Hu YW, Teng CJ, Tzeng CH, Yeh CM, Chen TJ, Lin JK, Lin CC, Lan YT, *et al*: Incidence of second primary malignancies following colorectal cancer: A distinct pattern of occurrence between colon and rectal cancers and association of co-morbidity with second primary malignancies in a population-based Cohort of 98,876 patients in Taiwan. *Medicine (Baltimore)* 94: e1079, 2015.
46. Hui D, Elsayem A, Li Z, De La Cruz M, Palmer JL and Bruera E: Antineoplastic therapy use in patients with advanced cancer admitted to an acute palliative care unit at a comprehensive cancer center: A simultaneous care model. *Cancer* 116: 2036-2043, 2010.
47. Beck JT: Potential role for mammalian target of rapamycin inhibitors as first-line therapy in hormone receptor-positive advanced breast cancer. *Onco Targets Ther* 8: 3629-3638, 2015.
48. Uhara H: Molecular target therapies for skin cancers. *Nihon Rinsho* 73: 1391-1397, 2015.
49. Oda K: Recent process of molecular target therapies in ovarian serous and endometrioid carcinomas on basis of integrated genomic characterization. *Gan To Kagaku Ryoho* 42: 169-173, 2015 (In Japanese).
50. Chen C, Fei Z, Chen L, Bai P, Lin X and Pan J: Will weight loss cause significant dosimetric changes of target volumes and organs at risk in nasopharyngeal carcinoma treated with intensity-modulated radiation therapy? *Med Dosim* 39: 34-37, 2014.
51. Liu SL, Han Y, Zhang Y, Xie CY, Wang EH, Miao Y, Li HY, Xu HT and Dai SD: Expression of metastasis-associated protein 2 (MAP2) might predict proliferation in non-small cell lung cancer. *Target Oncol* 7: 135-143, 2012.

52. Kim DS, Park KM, Won YS, Kim JY, Lee JK, Kim JG, Oh ST, Jung SS and Kang WK: Occurrence and prognosis of symptomatic venous thromboembolism in colorectal cancer surgery patients. *Vasc Specialist Int* 30: 49-55, 2014.
53. Wink KC, Belderbos JS, Dieleman EM, Rossi M, Rasch CR, Damhuis RA, Houben RM and Troost EG: Improved progression free survival for patients with diabetes and locally advanced non-small cell lung cancer (NSCLC) using metformin during concurrent chemoradiotherapy. *Radiother Oncol* 118: 453-459, 2016.
54. Charvat H, Sasazuki S, Inoue M, Iwasaki M, Sawada N, Shimazu T, Yamaji T and Tsugane S; JPHC Study Group: Prediction of the 10-year probability of gastric cancer occurrence in the Japanese population: The JPHC study cohort II. *Int J Cancer* 138: 320-331, 2016.
55. Shameem R, Hamid MS, Xu KY and Wu S: Comparative analysis of the effectiveness of abiraterone before and after docetaxel in patients with metastatic castration-resistant prostate cancer. *World J Clin Oncol* 6: 64-72, 2015.
56. Trinh XB, Tjalma WA, Vermeulen PB, Van den Eynden G, Van der Auwera I, Van Laere SJ, Helleman J, Berns EM, Dirix LY and van Dam PA: The VEGF pathway and the AKT/mTOR/p70S6K1 signalling pathway in human epithelial ovarian cancer. *Br J Cancer* 100: 971-978, 2009.
57. Zhu X, Song Y, Huo R, Zhang J, Sun S, He Y, Gao H, Zhang M, Sun X, Zhai T, *et al*: Cyr61 participates in the pathogenesis of rheumatoid arthritis by promoting proIL-1 $\beta$  production by fibroblast-like synoviocytes through an AKT-dependent NF- $\kappa$ B signaling pathway. *Clin Immunol* 157: 187-197, 2015.
58. Nakamura K, Nozawa K, Aoyagi Y, Ishihara S, Matsuda K, Fukushima J and Watanabe T: A case report of thyroid gland metastasis associated with lung metastasis from colon cancer. *Tumori* 97: 229-232, 2011.



This work is licensed under a Creative Commons Attribution-NonCommercial-NoDerivatives 4.0 International (CC BY-NC-ND 4.0) License.

RETRACTED